Skeletal muscle protein accretion rates and hindlimb growth are reduced in late gestation intrauterine growth-restricted fetal sheep

Paul J. Rozance[1] (ID), Laura Zastoupil[1], Stephanie R. Wesolowski[1], David A. Goldstrohm[1], Brittany Strahan[1], Melanie Cree-Green[1], Melinda Sheffield-Moore[2], Giacomo Meschia[1], William W. Hay Jr[1], Randall B. Wilkening[1] and Laura D. Brown[1] (ID)

[1] Department of Pediatrics, University of Colorado School of Medicine, Perinatal Research Center, Aurora, CO, USA
[2] Department of Internal Medicine, University of Texas Medical Branch, Division of Endocrinology, Galveston, TX, USA

The Journal of Physiology

Key points

- Adults who were affected by intrauterine growth restriction (IUGR) suffer from reductions in muscle mass, which may contribute to insulin resistance and the development of diabetes.
- We demonstrate slower hindlimb linear growth and muscle protein synthesis rates that match the reduced hindlimb blood flow and oxygen consumption rates in IUGR fetal sheep. These adaptations resulted in hindlimb blood flow rates in IUGR that were similar to control fetuses on a weight-specific basis.
- Net hindlimb glucose uptake and lactate output rates were similar between groups, whereas amino acid uptake was significantly lower in IUGR fetal sheep.
- Among all fetuses, blood O_2 saturation and plasma glucose, insulin and insulin-like growth factor-1 were positively associated and norepinephrine was negatively associated with hindlimb weight.
- These results further our understanding of the metabolic and hormonal adaptations to reduced oxygen and nutrient supply with placental insufficiency that develop to slow hindlimb growth and muscle protein accretion.

Abstract Reduced skeletal muscle mass in the fetus with intrauterine growth restriction (IUGR) persists into adulthood and may contribute to increased metabolic disease risk. To determine how placental insufficiency with reduced oxygen and nutrient supply to the fetus affects hindlimb blood flow, substrate uptake and protein accretion rates in skeletal muscle, late gestation control (CON) ($n = 8$) and IUGR ($n = 13$) fetal sheep were catheterized with aortic and femoral catheters and a flow transducer around the external iliac artery. Muscle protein kinetic rates were measured using isotopic tracers. Hindlimb weight, linear growth rate, muscle protein accretion rate and fractional synthetic rate were lower in IUGR compared to CON ($P < 0.05$). Absolute hindlimb blood flow was reduced in IUGR (IUGR: 32.9 ± 5.6 ml min^{-1}; CON: 60.9 ± 6.5 ml min^{-1}; $P < 0.005$), although flow normalized to hindlimb weight was similar between groups. Hindlimb oxygen consumption rate was lower in IUGR (IUGR: 10.4 ± 1.4 μmol min^{-1} 100 g^{-1}; CON: 14.7 ± 1.3 μmol min^{-1} 100 g^{-1}; $P < 0.05$). Hindlimb glucose uptake and lactate output rates were similar between groups, whereas amino acid uptake was lower in IUGR (IUGR: 1.3 ± 0.5 μmol min^{-1} 100 g^{-1}; CON: 2.9 ± 0.2 μmol min^{-1} 100 g^{-1}; $P < 0.05$). Blood O_2 saturation ($r^2 = 0.80$, $P < 0.0001$) and plasma glucose ($r^2 = 0.68$, $P < 0.0001$), insulin ($r^2 = 0.40$, $P < 0.005$) and insulin-like growth factor (IGF)-1 ($r^2 = 0.80$, $P < 0.0001$) were positively associated and norepinephrine ($r^2 = 0.59$, $P < 0.0001$) was negatively associated with hindlimb weight. Slower hindlimb linear growth and muscle protein synthesis rates match reduced hindlimb blood flow and oxygen consumption rates in the IUGR fetus. Metabolic adaptations to slow

hindlimb growth are probably hormonally-mediated by mechanisms that include increased fetal norepinephrine and reduced IGF-1 and insulin.

Abbreviations   CON, control; IGF, insulin-like growth factor; FDS, flexor digitorum superficialis; FSR, fractional muscle protein synthetic rate; IUGR, intrauterine growth restriction; KIC, α-ketoisocaproic acid; t-BDMS, N-tert-butyldimethylsilyl-N-methyltrifluoroacetamide.

Introduction

Reduced muscle growth *in utero* has a negative impact on the amount of muscle mass an individual has in adulthood, which may contribute to increased metabolic disease risk. Skeletal muscle mass is lower in the fetus and neonate exposed to placental insufficiency-induced intrauterine growth restriction (IUGR) (Yau & Chang, 1993; Padoan *et al.* 2004; Larciprete *et al.* 2005). A large number of epidemiological studies show that birthweight, when used as an index of the effect of the intrauterine environment on fetal growth, is positively correlated with lean mass in adulthood (Brown & Hay, 2016). As an example, a slower trajectory of muscle growth during childhood was observed in children who were born small for gestational age compared to those children who were born with an appropriate birth weight (Baker *et al.* 2010).

IUGR from placental insufficiency is a condition characterized by several potential mechanisms that could independently or interactively regulate skeletal muscle growth, including low fetal blood oxygen content (Pardi *et al.* 1993, 2002), lower fetal glucose, insulin and insulin-like growth factor (IGF)-1 concentrations (Economides *et al.* 1989; Marconi *et al.* 1996; Tzschoppe *et al.* 2015), and higher fetal norepinephrine concentrations (Greenough *et al.* 1990). In a sheep model of placental insufficiency and IUGR, we demonstrated that skeletal muscle mass in the late gestation IUGR fetus was disproportionately lower when normalized to either bone length or brain weight compared to control fetal sheep (Soto *et al.* 2017). IUGR fetuses also have a lower partial pressure of oxygen (P_{aO_2}) by mid-gestation (Arroyo *et al.* 2008), which progresses to lower oxygen contents, oxygen saturations (S_{aO_2}) and oxygen consumption rates by late gestation (Regnault *et al.* 2007; Brown *et al.* 2012). The fetal hemodynamic response to acute hypoxaemia, which includes peripheral vasoconstriction and reduced femoral arterial blood flow (Boyle *et al.* 1992; Newman *et al.* 2000), indicates that preferential restrictions in skeletal muscle growth may be mediated by reduced blood flow and oxygen delivery. However, fetal responses to chronic hypoxaemia include mechanisms that down-regulate fetal growth to adapt to a reduction in the normal gestational increase of oxygen supply (Akalin-Sel & Campbell, 1992; Gardner *et al.* 2003; Brain *et al.* 2015; Poudel *et al.* 2015; Allison *et al.* 2016). Studies aiming to determine the mechanisms underlying lower rates of muscle growth in IUGR fetuses resulting from chronic placental insufficiency have not included a comprehensive analysis of blood flow, nutrient uptake rates and protein metabolism within the fetal hindlimb and skeletal musculature.

The primary goal of the present study was to determine the differences in hindlimb growth rates, skeletal muscle protein metabolic rates, and substrate and oxygen uptake rates between normally growing control and IUGR fetal sheep. We also explored the potential physiological mechanisms that could be responsible for establishing hindlimb weight by late gestation. We measured the blood flow and net uptake rates of oxygen, glucose, lactate and amino acids by the fetal hindlimb and used novel tracer methodology to determine skeletal muscle protein metabolic rates in a well-established sheep model of IUGR induced by placental insufficiency (Bell *et al.* 1987; Wilkening *et al.* 1994). We hypothesized that the IUGR fetus would demonstrate slower rates of hindlimb linear growth, net protein uptake, and skeletal muscle protein synthesis and accretion and that these would match the reduced blood flow and oxygen delivery to the hindlimb.

Methods

Ethical approval

Study protocols were approved by the Institutional Animal Care and Use Committee at the University of Colorado Anschutz Medical Campus (Protocol #77614101E) and follow the guidelines from the American Association for the Accreditation of Laboratory Animal Care. Pregnant Columbia-Rambouillet mixed-breed sheep were housed in an environmental chamber with elevated ambient temperatures (40°C for 12 h; 35°C for 12 h) and 40% humidity alongside other sheep from 38 days of gestation (dga) (term = 147 dga) to 116 dga to produce placental insufficiency and intrauterine growth restriction (IUGR group; $n = 13$) (Bell *et al.* 1987; Brown *et al.* 2012). Control ewes were housed in the same environmental chamber but with normal ambient temperatures and humidity

from 43 dga to 120 dga (CON group; $n = 8$). After environmental treatment, all sheep were housed in normal ambient temperatures and humidity for the remainder of the studies. All sheep were given *ad libitum* access to water. Maternal feed intake was matched on an absolute basis between sheep in CON and IUGR groups and no sheep consumed less than that recommended by the National Research Council. All sheep were pregnant with singletons, with the exception of one triplet pregnancy in the IUGR group, which was found incidentally at the time of animal death. Only one of the triplet fetuses was catheterized, studied and included in the analysis. This triplet fetus was not an outlier for any measurement. Fetal weights for all three triplets were relatively consistent and demonstrated 56–63% growth restriction compared to mean CON fetal weight (the weight of the triplet included in the analysis was 1466 g; the weights of the other two triplets were 1230 g and 1528 g).

Pregnant sheep at 126–128 dga underwent a surgical procedure for fetal and maternal catheter placement in accordance with previously published methods (Wilkening *et al.* 1994; Brown *et al.* 2012). Sheep were fasted for 24 h and thirsted for 12 h prior to surgery. A superficial maternal vein was used to administer diazepam (0.2 mg kg^{-1}) and ketamine (20 mg kg^{-1}) for induction and sheep were maintained on isoflurane inhalation anaesthesia (2–4%) for the duration of the surgical procedure. The depth of anaesthesia was determined and maintained by response to toe pinch, corneal reflex, assessment of jaw tone in the mother and muscle tone in the fetus, as well as continuous pulse oximetry and heart rate monitoring. The fetal lamb was exposed by maternal laparotomy and hysterotomy. Polyvinyl catheters were placed in the pedal artery with the tip positioned in the external iliac artery and in the saphenous vein with the tip positioned in the distal inferior vena cava. The hindlimb length was measured from the femoral head to the top edge of the hoof. In addition, a small skin incision was made over the lateral thigh and a 0.5-cm^3 biopsy was obtained from the biceps femoris muscle and frozen in liquid nitrogen. This limb was designated the 'non-study' limb.

In the contralateral hindlimb designated the 'study' limb, a catheter was placed in the pudendoepigastric venous trunk with the tip advanced 2 cm into the external iliac vein. The deep circumflex iliac artery and vein and the pudendoepigastric arterial trunk were ligated to minimize collateral circulation to midline structures that might contaminate external iliac blood flow to the skin, bone and muscle of the hindlimb. A 3-mm transit time ultrasonic blood flow transducer (Transonic Systems, Ithaca, NY, USA) was positioned around the external iliac artery of the study limb for continuous blood flow measurement. A distal arterial occluder was placed for zero-flow corrections. The catheters, flow probe and occluder were tunnelled s.c. to the maternal flank. Post-surgical care included frequent monitoring of feed and water intake, surgical wound inspection and analgesia with intramuscular injection of banamine (1.1 mg kg^{-1}).

Metabolic study

Post-surgical recovery was a minimum of 6 days before performing tracer metabolic studies, which were performed at 133–136 dga. Blood samples from the external iliac artery and vein were simultaneously obtained at time zero. Two isotopomers of phenylalanine, ring ^{2,3,3} ^{2}H$_8$ ($m+8$) and ring ^{2}H$_5$ ($m+5$) were started 6 h apart and infused overnight at a rate of 0.3 μmol min^{-1} kg^{-1} based on estimated fetal weight (Cambridge Isotope Laboratories, Andover, MA, USA). The multiple infusion start time method (Brown *et al.* 2009) staggers the start time of $m + 5$ and $m + 8$ phenylalanine to measure the fractional muscle protein synthetic rate (FSR) with only one muscle biopsy. The next day, a primed (30 μmol kg^{-1}) infusion of 1-^{13}C leucine (Cambridge) was administered at a rate of 0.5 μmol min^{-1} kg^{-1} estimated fetal weight to measure muscle protein kinetics using a three pool model (Biolo *et al.* 1992). Three hours later, four blood draws from the external iliac artery and vein were simultaneously obtained over 1 h to establish steady-state conditions for net hindlimb substrate uptake rate calculations. External iliac blood flow measurements were hand recorded during each of the four blood draws and averaged to represent the flow during the sampling period. An isovolemic transfusion of heparinized maternal blood (24 ml) was administered to the fetus during the sampling period to replace fetal blood removed. Flow probe malfunction occurred in two of the 13 IUGR fetuses and phenylalanine tracers infiltrated in one of the IUGR fetuses, leaving 11 IUGR fetuses available for the leucine tracer metabolic study and 12 IUGR fetuses available for FSR measurements.

Fetal skeletal muscle collection

After conclusion of the metabolic study, ewes received diazepam (0.2 mg kg^{-1}) and ketamine (20 mg kg^{-1}) I.V. and fetuses were delivered via maternal laparotomy and hysterotomy. The biceps femoris muscle was exposed from the 'study' hindlimb and a biopsy was obtained from the anaesthetized fetus and immediately frozen in liquid nitrogen. I.V. pentobarbital sodium (Fatal Plus; Bortech Parmaceuticals, Dearborn, MI, USA) was administered to both the mother and the fetus, after which placental, fetal (whole body), fetal organ and fetal length measurements were obtained. The 'non-study' hindlimb was disarticulated and weighed. Fetal hindlimb muscles including the biceps femoris, flexor digitorum

superficialis (FDS), tibialis anterior, gastrocnemius and extensor digitorum longus were weighed. Muscle mid-bellies from the biceps femoris, tibialis anterior and FDS muscles were placed on corkboard thinly coated with optimal cutting temperature media, frozen in liquid nitrogen-cooled isopentane for 60 s and stored at −70°C.

Fetal blood sample measurements

Fetal blood was analysed for measurements of pH, P_{aCO_2}, P_{aO_2}, S_{aO_2}, O_2 content and haematocrit using a blood gas analyser (Radiometer, Copenhagen, Denmark). Plasma samples were used for measuring concentrations of glucose and lactate (model 2700; Yellow Springs Instrument, Yellow Springs, OH, USA). Plasma arterial insulin, IGF-1 and cortisol concentrations were measured by an enzyme-linked immunosorbent assay as described previously (Soto *et al.* 2017). Plasma amino acid and norepinephrine concentrations were measured using HPLC as described previously (Brown *et al.* 2012).

Plasma enrichments of leucine, phenylalanine and α-ketoisocaproic acid (KIC) and whole blood enrichments of CO_2 were measured as described previously (Rozance *et al.* 2009*a*) with slight modification: plasma (0.05 ml) was added to 0.15 ml of 50% acetic acid. Cation exchange resin (AG-50, H^+ form at 0.05 ml) was added and contaminants were removed using three washes of 1 ml of 70% isopropanol in water. Leucine and phenylalanine were eluted using 0.6 ml of 5 N ammonium hydroxide. The ammonium hydroxide eluent was dried under reduced pressure and plasma leucine and phenylalanine isotopic enrichments were measured after conversion to a *N*-tert-butyldimethylsilyl-*N*-methyltrifluoroacetamide (t-BDMS) derivative (0.05 ml of 1:1 50% t-BDMS with 1% tert-butyldimethylchlorosilane in anhydrous acetonitrile incubated at 63°C for 1 h). The leucine isotopic enrichment was determined at m/z 303/302 and the phenylalanine isotopic enrichments were determined at m/z 313/308 ($m + 5$) and m/z 316/308 ($m + 8$) using the selective ion monitoring method.

For KIC enrichment, 0.05 ml of plasma was diluted in 0.1 ml water and KIC was reduced to α-hydroxycaproic acid with sodium borohydride (0.025 ml, 10 mg ml^{-1} in water at room temperature for 15 min). The reaction was terminated by the addition of 0.025 ml of 4 N HCl. Ethyl acetate (1 ml) was added, washed with 0.5 ml of 0.04 M HCl and the organic solvent was removed under reduced pressure. Plasma KIC isotopic enrichment was measured after conversion to a α-hydroxycaproic acid t-BDMS derivative at 85°C for 20 min. The KIC isotopic enrichment was determined at m/z 304/303.

For whole blood $^{13}CO_2$ enrichment, 0.03 ml concentrated phosphoric acid (85% in water) was purged with ultra-high purity helium for 5 min in an Exetainer tube (Labco, Lampeter, UK). Whole blood was added (0.2 ml)

and CO_2 was allowed to equilibrate between the sample and the pure headspace gas for a minimum of 24 h and at a constant temperature of 30°C. Gas headspace analysis was processed through a GC Pal autosampler (Leap Technologies, Fort Lauderdale, FL, USA) and the captured gas was passed through a gas chromatograph column with helium as the carrier gas and introduced to the isotope ratio mass spectrometer (Delta V, Thermo Electron, Bremen, Germany). Standard gas (ultra-high purity CO_2) was sampled five times prior to each sample being measured. Excess $^{13}CO_2$ (AT% excess) was calculated relative to baseline CO_2.

Enrichment within the intracellular and protein bound compartments of skeletal muscle

Separation of the intracellular and protein-bound compartments of fetal sheep muscle has been adapted from methods reported previously (Calder *et al.* 1992). Biceps femoris muscle (50 mg) obtained at the time of fetal surgery (pre-tracer infusion) and at the time of tissue collection (post-tracer infusion) was separated into intracellular and protein-bound compartments by homogenization in 0.8 ml of 10% perchloric acid and centrifugation at 16 100 g for 5 min at 4°C. The intracellular-containing supernatant was separated. The protein-bound fraction was washed with 0.8 ml of 10% perchloric acid and centrifuged. The additional intracellular supernatant fraction was pooled with the original fraction and frozen at −80°C. The protein-bound fraction then was washed 0.8 ml of 2% perchloric acid (twice) and 0.8 ml of 100% methanol (three times) using a handheld homogenizer and dried overnight at 50°C. Dry weight was recorded and the protein-bound fraction was hydrolysed with 3 ml of 6 N HCl at 110°C for 24 h in Teflon line screw cap glass tubes. Upon acid hydrolysis, a volume containing 1 mg of the previously dried protein was dried under reduced pressure. After drying, phenylalanine in the protein-bound fraction was decarboxylated to phenylethylamine using 1 mg of tyrosine decarboxylase and 0.25 mg of pyridoxal phosphate in 0.5 M sodium citrate, pH 6.3 at 50°C for 17 h. Contaminants were removed using aqueous NaOH washes in chloroform. Phenylethylamine was extracted using 1 N HCl and dried under reduced pressure.

Phenylethylamine isotopic enrichments were determined at m/z 183/180 and $(185 + 186)/180$. To measure low levels of protein-bound enrichment, $m + 2$ (m/z 180) was used as the reference ion instead of $m + 0$ (m/z 178). To incorporate any potential loss in enrichment as a result of hydrogen exchange with pyridoxal phosphate during the decarboxylation reaction, the sum of $m + 7$ (m/z 185) and $m + 8$ (m/z of 186) enrichments was used. Measured protein-bound isotope enrichments were compared with enzymatically

decarboxylated $m + 5$, $m + 7$ and $m + 8$ phenylalanine standards to avoid concentration-dependent changes in the observed enrichments. For intracellular processing, leucine and phenylalanine from the previously frozen fraction were isolated using cation exchange resin (AG-50; Bio-Rad, Hercules, CA, USA) (H^+ form, 1.4 ml). Contaminants were removed using 20 ml of water. Leucine and phenylalanine were eluted using 1.8 ml of 5 N ammonium hydroxide and dried under reduced pressure. The leucine ($m + 1$) and phenylalanine ($m + 5$, $m + 8$) isotopic enrichments were determined at m/z 303/302, 313/308 and 316/308, respectively. Naturally occurring ^{13}C ($m + 1$) in pre-infused plasma and muscle pools was subtracted from post-infused values. We did not detect any naturally occurring $^{2,3,3}{}^2H_8$ or $^2H_5$ ($m + 5$, $m + 8$) in plasma or muscle pools.

Calculations

Hindlimb linear growth rate was calculated by subtracting the lower extremity hindlimb growth measurements obtained at the time of surgery and at the time of animal death and dividing by the intervening days. Plasma hindlimb blood flow was calculated by multiplying hindlimb blood flow by (1 − hct). Hindlimb (net) oxygen, glucose, lactate and amino acid uptake rates were calculated by multiplying the mean arterial–venous (a − v) concentration difference from the four steady-state blood draws by the mean hindlimb blood flow during the draw period. The uptake rates of individual amino acids were summed to calculate the total amino acid uptake rate. Oxygen delivery was calculated by multiplying the arterial oxygen content by hindlimb blood flow. Nutrient-oxygen quotients were determined by dividing the whole blood a–v difference in substrate by the a–v difference in oxygen content, multiplied by the number of oxygen molecules needed to oxidize one molecule of the nutrient (Regnault *et al.* 2013). Net nitrogen and carbon uptake rates are the sum of each measured substrate (amino acid, glucose and lactate) multiplied by their respective number of nitrogen or carbon atoms.

All hindlimb substrate uptake rates were normalized to 100 g of fetal hindlimb weight and compared between CON and IUGR groups. In a separate but contemporary group of late gestation CON ($n = 8$; hindlimb weight 305 ± 7 g) and IUGR ($n = 6$; hindlimb weight 146 ± 11 g) fetal sheep, we found similar relative proportions of muscle weight per hindlimb weight (CON: muscle $34 \pm 0.01\%$, connective tissue $27 \pm 0.01\%$, skin $24 \pm 0.01\%$ and bone $10 \pm 0.00\%$; IUGR: muscle $33 \pm 0.02\%$, connective tissue $27 \pm 0.02\%$, skin $23 \pm 0.01\%$ and bone $10 \pm 0.01\%$).

Muscle protein metabolic rates, using a three pool model with 1-^{13}C-leucine as the tracer, were calculated using the equations shown in Table 1 (Biolo *et al.* 1992). We chose 1-^{13}C-leucine to measure leucine oxidation by the hindlimb, in addition to synthesis and breakdown rates. The three-pool model of leucine metabolism is based on the fact that skeletal muscle is the primary site of protein metabolism and leucine oxidation (Biolo *et al.* 1994; Wolfe & Chinkes, 2005; Brosnan & Brosnan, 2006).

FSR were calculated using the equation:

$$[E_{P(m+8)}/E_{M(m+8)} \ - \ E_{P(m+5)}/E_{M(m+5)}]/\Delta_t$$

where E_M and E_P are enrichments in the intracellular and protein bound compartment of muscle, respectively, and Δ_t is the time between $m + 8$ and $m + 5$ phenylalanine isotope infusion start times.

Immunohistochemistry

Isopentane-preserved biceps femoris, tibialis anterior and FDS muscles were removed from corkboard and 10-μm sections were prepared as described previously (Soto *et al.* 2017). Muscle sections were incubated with the following antibodies: anti-laminin rabbit polyclonal IgG (dilution 1:100; Sigma-Aldrich, St Louis, MO, USA), anti-myosin heavy chain (MHC) Type I (slow) mouse monoclonal IgG (dilution 1:20; Abcam, Cambridge, MA, USA) and anti-MHC Type IIa mouse IgG (dilution 1:2; a gift from Dr Leslie Leinwand, University of Colorado Boulder, Boulder, CO, USA). Immunocomplexes were detected with AMCA donkey anti-rabbit IgG (dilution 1:250; Jackson ImmunoResearch, West Grove, PA, USA) and Cy2 donkey anti-mouse IgG (dilution 1:250; Jackson ImmunoResearch). Fluorescence images were visualized and fibre type-specific cross-sectional areas were measured using the Count and Measure module within CellSens Dimension Imaging Software (Olympus America Inc., Center Valley, PA, USA) and averaged from a minimum of 250 fibres per fetus.

Statistical analysis

Unpaired Student's *t* tests were used for direct comparisons between CON and IUGR groups (Prism, version 5; GraphPad Software Inc., San Diego, CA, USA). A Mann–Whitney test was used when variances were unequal. Two-way ANOVA was used to determine the effect of group (CON and IUGR) and myofibre type (Type I and Type IIa) on myofibre area. The effect of sex was determined by two-way ANOVA with terms for group (CON and IUGR), sex and their interaction. Relationships between various parameters and fetal hindlimb weight were determined with simple linear regression analysis because values were normally distributed. Norepinephrine and IGF-1 were log transformed for

Table 1. Fetal skeletal muscle protein metabolic rates

Flux rates (μmol min^{-1} 100 g^{-1})	Equation	CON ($n = 8$)	IUGR ($n = 11$)	P
Net Leu uptake rate	$(CLeu_A - CLeu_V) \times PF$	0.28 ± 0.02	0.20 ± 0.02	<0.05
Net KIC uptake rate	$(CKIC_A - CKIC_V) \times PF$	0.03 ± 0.02	-0.00 ± 0.01	0.06
Inward Leu transport rate ($F_{M,A}$)	$\{[(ELeu_M - ELeu_V/ELeu_A - ELeu_M) \times CLeu_V] + CLeu_A\} \times PF$	0.95 ± 0.91	0.64 ± 0.07	<0.05
Outward Leu transport rate ($F_{V,M}$)	$\{[(ELeu_M - ELeu_V/ELeu_A - ELeu_M) \times CLeu_V] + CLeu_V\} \times PF$	0.68 ± 0.08	0.50 ± 0.05	0.06
Intracellular Leu utilization rate	$[(CLeu_A \times ELeu_A) - (CLeu_V \times ELeu_V)] \times PF/ELeu_M$	0.57 ± 0.05	0.39 ± 0.06	<0.05
Protein breakdown rate	Intracellular Leu utilization rate – Net Leu uptake rate	0.28 ± 0.04	0.19 ± 0.04	0.1
Leu oxidation rate	$[(CCO_{2V} \times ECO_{2V}) - (CCO_{2A} \times ECO_{2A})] \times BF/EKIC_A$	0.15 ± 0.02	0.12 ± 0.02	0.3
Leu oxidation fraction	Leu oxidation rate/Intracellular Leu utilization rate	0.27 ± 0.03	0.35 ± 0.04	0.2
Protein synthesis rate	Intracellular utilization – Leu oxidation rate	0.42 ± 0.04	0.27 ± 0.05	<0.05
Protein accretion rate	Net Leu uptake rate + Net KIC uptake rate – Leu oxidation rate	0.17 ± 0.03	0.08 ± 0.02	<0.05

Values are the mean $\pm$ SEM. P values are from Student's t tests or the Mann–Whitney test. All rates are μmol min^{-1} 100 g hindlimb weight^{-1}.
PF, external iliac arterial plasma flow; BF, external iliac blood flow. $F_{X,Y}$ refers to the rate of flow of leucine from pool y to pool x, where A, M, and V represent artery, muscle and vein, respectively. C_A and C_V are plasma concentrations and E_A and E_V are enrichments in the external iliac artery and femoral vein, respectively.

regression analysis. $P \leq 0.05$ was considered statistically significant.

Results

Placental and fetal weights

Maternal, placental, fetal (whole body) and fetal muscle weights and linear measurements are shown in Table 2. Maternal weights at time of surgery and maternal feed intake were similar. Placentomes in IUGR weighed 42% less than CON placentas ($P < 0.01$). Fetal whole body weights were 41% lower ($P < 0.0005$), fetal hindlimb weights were 46% lower ($P < 0.0001$) and brain weights were 14% lower ($P < 0.005$) in IUGR compared to CON. The percentage of brain weight relative to fetal weight was higher in IUGR compared to CON ($P < 0.005$). The percentage of hindlimb weight relative to fetal weight in IUGR was lower than CON ($P < 0.005$). Crown–rump lengths were 12% shorter ($P < 0.01$) and hindlimb lengths were 22% shorter in IUGR ($P < 0.0001$). Individual hindlimb muscle weights were lower in IUGR compared to CON, with 45–48% lower absolute weights and 29–38% lower weights relative to lower extremity hindlimb lengths ($P < 0.05$) (Table 2). There were some minor differences in placental and fetal weights between male and female fetuses. Placental weight tended to be lower in females compared to males ($P = 0.06$) and the weight of the FDS muscle was lower in females ($P < 0.05$), without significant interactions between CON and IUGR groups.

Fetal blood gas, substrate and hormone concentrations

Fetal blood gas values and substrate and hormone concentrations are shown in Table 3. Fetal arterial blood P_{aO_2}, O_2 saturation and O_2 content were lower in IUGR compared to CON ($P < 0.001$). Fetal plasma glucose concentrations were 30% lower ($P < 0.0005$) and fetal plasma lactate concentrations tended to be higher ($P = 0.06$) in IUGR compared to CON. Minimal differences were observed in plasma amino acid concentrations, with the exception of taurine (65% higher, $P < 0.01$), alanine (35% higher, $P < 0.05$), tyrosine (26% less, $P < 0.0005$) and arginine (41% less, $P < 0.005$) in IUGR compared to CON (Table 3). Insulin and IGF-1 concentrations were 65% and 60% lower, respectively, in IUGR $vs.$ CON ($P < 0.005$ for each). Fetal plasma norepinephrine concentrations were six-fold higher in IUGR $vs.$ CON ($P < 0.05$). Fetal sex had no effect on fetal substrate and hormone concentrations, with the exception of insulin (higher in females, $P < 0.05$), as well as serine, methionine and arginine concentrations (lower in females, $P < 0.05$), without a significant interaction between CON and IUGR groups.

**Table 2. Maternal, placental, and fetal weights at time of study**

	Control ($n = 8$)	IUGR ($n = 13$)	P
Maternal and fetal measurements			
Maternal weight at surgery (kg)	62 ± 2	59 ± 3	0.6
Maternal feed intake (kg day^{-1})	1.6 ± 0.1	1.4 ± 0.1	0.2
Gestational age (days)	134 ± 0	134 ± 0	0.5
% male	50%	54%	
Placental weight (g)	320 ± 38	185 ± 24	<0.01
Fetal weight (g)	3324 ± 137	1961 ± 188	<0.0005
Brain weight (g)	50.2 ± 1.3	43.3 ± 1.2	<0.005
Hindlimb weight (g)	344 ± 17	185 ± 19	<0.0001
Brain relative to fetal weight (%)	15.2 ± 0.5	24.1 ± 1.9	<0.005
Hindlimb relative to fetal weight (%)	10.3 ± 0.2	9.4 ± 0.1	<0.005
Crown–rump length (cm)	47.8 ± 1.0	42.0 ± 1.3	<0.01
Hindlimb length (cm)	37.0 ± 0.8	29.0 ± 1.1	<0.0001
Fetal hindlimb muscle weights			
Biceps femoris (g)	18.1 ± 0.7	9.9 ± 1.0	<0.0001
per hindlimb length (g cm^{-1})	0.49 ± 0.01	0.33 ± 0.02	<0.0005
per fetal weight (g kg^{-1})	5.5 ± 0.1	5.1 ± 0.2	<0.05
Gastrocnemius (g)	9.1 ± 0.4	5.0 ± 0.5	<0.0001
per hindlimb length (g cm^{-1})	0.24 ± 0.01	0.17 ± 0.01	<0.0005
per fetal weight (g kg^{-1})	2.7 ± 0.1	2.5 ± 0.1	0.1
Tibialis anterior (g)	4.0 ± 0.3	2.1 ± 0.3	<0.0005
per hindlimb length (g cm^{-1})	0.11 ± 0.01	0.07 ± 0.01	<0.005
per fetal weight (g kg^{-1})	1.2 ± 0.1	1.0 ± 0.1	<0.05
Flexor digitorum superficialis (g)	3.1 ± 0.3	1.6 ± 0.2	<0.0005
per hindlimb length (g cm^{-1})	0.08 ± 0.01	0.05 ± 0.01	<0.001
per fetal weight (g kg^{-1})	0.93 ± 0.04	0.77 ± 0.04	<0.05
Extensor digitorum longus (g)	1.1 ± 0.1	0.6 ± 0.1	<0.005
per hindlimb length (g cm^{-1})	0.03 ± 0.002	0.02 ± 0.003	<0.05
per fetal weight (g kg^{-1})	0.34 ± 0.02	0.31 ± 0.03	0.4

Values are the mean ± SEM. P values from Student's t tests or the Mann–Whitney test are shown.

Fetal hindlimb blood flow and net hindlimb substrate uptake rates

External iliac blood flow to the hindlimb was 46% lower in IUGR compared to CON ($P < 0.005$) but, when normalized to hindlimb weight, blood flow was similar between groups (Fig. 1). Weight-specific oxygen delivery to the hindlimb was 40% lower in IUGR ($P < 0.05$) (Fig. 2A). Oxygen consumption rate by the hindlimb was 29% lower in IUGR ($P < 0.05$) (Fig. 2B). Weight-specific net glucose uptake rate ($P = 0.12$) and net lactate output rate by the hindlimb did not differ statistically between groups (Fig. 2C and D). Glucose extraction efficiency was similar between groups (IUGR 19.9 ± 1.1, CON 17.0 ± 1.2%; $P = 0.1$) and oxygen extraction efficiency was higher in IUGR (IUGR 35.5 ± 2.3, CON 26.6 ± 1.7%; $P < 0.05$). Weight-specific net total amino acid uptake rate by the hindlimb was 55% lower in IUGR compared to CON ($P < 0.01$) (Fig. 2E). Net total amino acid uptake rate correlated with hindlimb weight ($r^2 = 0.85$, $P < 0.0001$) (Fig. 2F). Net total carbon uptake rate was 42% lower (IUGR 14.3 ± 3.2 μmol min^{-1} 100 g^{-1} hindlimb, CON 24.8 ± 1.7; $P < 0.05$) and net total nitrogen uptake rate was 53% lower (IUGR 1.9 ± 0.6 μmol min^{-1} 100 g^{-1} hindlimb, CON 4.0 ± 0.3; $P < 0.05$) in IUGR compared to CON.
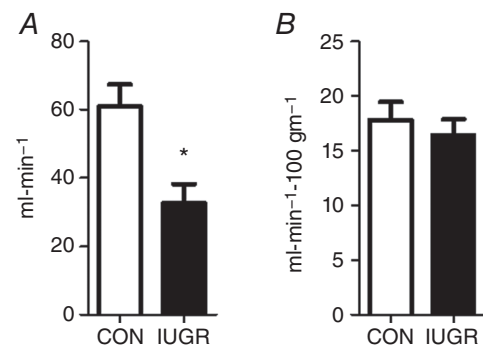
Figure 1. Fetal hindlimb blood flow
External iliac blood flow was measured in CON (white bars, $n = 8$) and IUGR (black bars, $n = 11$) fetal sheep at 134 days of gestation. A, absolute blood flow. B, blood flow normalized to 100 g of hindlimb weight. Values represent the mean ± SEM. *$P < 0.005$ by Student's t test.

Table 3. Fetal blood gas, substrate and hormone measurements

	Comparison of means			Correlation with hindlimb weight	
	Control	IUGR	*P*	r^2	*P*
Blood gas measurements					
pH	7.36 ± 0.00	7.34 ± 0.01	< 0.05	0.49 (+)	< 0.0005
P_{aCO_2} (mmHg)	50.4 ± 0.7	51.5 ± 0.7	0.3	0.06	0.3
P_{aO_2} (mmHg)	20.6 ± 0.7	14.6 ± 0.9	<0.0005	0.63 (+)	<0.0001
S_{aO_2} (%)	48.3 ± 1.8	26.6 ± 3.2	<0.0005	0.80 (+)	<0.0001
O_2 content (mmol L^{-1})	3.3 ± 0.2	1.9 ± 0.3	<0.01	0.75 (+)	<0.0001
Hct (%)	34.1 ± 1.0	34.2 ± 1.4	0.9	0.10	0.2
Plasma substrates					
Glucose (mg dL^{-1})	17.9 ± 0.5	12.6 ± 1.0	<0.0005	0.68 (+)	<0.0001
Lactate (mmol L^{-1})	2.0 ± 0.1	2.6 ± 0.2	0.06	0.18	0.06
Taurine (μmol L^{-1})	49.5 ± 9.7	139.5 ± 32.4	<0.01	0.23 (−)	<0.05
Aspartate (μmol L^{-1})	14.0 ± 1.5	12.5 ± 1.6	0.5	0.11	0.1
Threonine (μmol L^{-1})	276.3 ± 42.8	235.8 ± 25.1	0.4	0.02	0.6
Serine (μmol L^{-1})	354.0 ± 16.2	460.3 ± 65.3	0.5	0.00	0.9
Asparagine (μmol L^{-1})	34.8 ± 2.0	52.4 ± 11.2	0.1	0.15	0.08
Glutamate (μmol L^{-1})	31.8 ± 2.7	29.5 ± 2.7	0.6	0.09	0.2
Glutamine (μmol L^{-1})	397.2 ± 44.3	379.8 ± 18.4	0.7	0.01	0.7
Proline (μmol L^{-1})	111.2 ± 13.8	133.2 ± 10.2	0.2	0.20 (−)	<0.05
Glycine (μmol L^{-1})	288.9 ± 21.0	371.2 ± 33.3	0.09	0.13	0.1
Alanine (μmol L^{-1})	228.7 ± 15.0	309.6 ± 20.1	<0.05	0.33 (−)	<0.01
Valine (μmol L^{-1})	322.5 ± 33.5	336.4 ± 20.8	0.7	0.01	0.6
Cysteine (μmol L^{-1})	11.8 ± 1.6	14.5 ± 1.9	0.3	0.15	0.1
Methionine (μmol L^{-1})	82.2 ± 7.3	68.4 ± 7.0	0.2	0.29 (+)	<0.05
Isoleucine (μmol L^{-1})	83.0 ± 4.0	68.6 ± 18.6	0.06	0.22 (+)	<0.05
Leucine (μmol L^{-1})	145.8 ± 15.2	153.5 ± 12.5	0.7	0.02	0.6
Tyrosine (μmol L^{-1})	131.3 ± 6.6	96.6 ± 4.7	<0.0005	0.37 (+)	<0.005
Phenylalanine (μmol L^{-1})	160.3 ± 15.3	179.2 ± 8.6	0.3	0.10	0.2
Tryptophan (μmol L^{-1})	39.1 ± 2.4	37.0 ± 1.3	0.4	0.11	0.1
Ornithine (μmol L^{-1})	76.7 ± 6.6	81.7 ± 7.3	0.6	0.07	0.2
Lysine (μmol L^{-1})	59.0 ± 5.8	77.0 ± 7.2	0.1	0.04	0.4
Histidine (μmol L^{-1})	53.1 ± 4.4	53.6 ± 3.4	0.9	0.01	0.8
Arginine (μmol L^{-1})	91.2 ± 9.0	53.5 ± 5.7	<0.005	0.65 (+)	<0.0001
Plasma hormone concentrations					
Insulin (ng ml^{-1})[a]	0.40 ± 0.09	0.14 ± 0.02	<0.005	0.40 (+)	<0.005
IGF-1 (ng ml^{-1})[a]	108.2 ± 15.2	43.6 ± 9.5	<0.005	0.80[a] (+)	<0.0001
Cortisol (ng ml^{-1})	20.2 ± 5.3	25.3 ± 5.3	0.5	0.01	0.6
Norepinephrine (pg ml^{-1})[a,b]	617 ± 253	4313 ± 1960	<0.005	0.59 (−)	<0.0001

Values are the mean ± SEM. *P* values from Student's *t* tests or the Mann–Whitney tests are shown. [a]Concentrations were log transformed for correlation analysis. [b]Concentrations were log transformed for comparison of means. Correlations are between blood gas, substrate or hormone measurements and hindlimb weight. Correlation coefficients are noted as (+) and (−) to indicate positive and negative correlations, respectively. [Corrections made on 20 November 2017 after first online publication: Except for Glucose and Lactate, unit for all other Plasma substrates was corrected from nmol L^{-1} to μmol L^{-1}]

Muscle protein metabolism and myofibre area

Comparisons of CON and IUGR protein metabolic rates are shown in Table 1. Net inward ($P < 0.05$) and outward ($P = 0.06$) leucine transport rates were 33% and 26% lower, respectively, in IUGR compared to CON. The intracellular leucine utilization rate, or the rate of leucine used within the intracellular compartment for either protein synthesis or oxidation, was 32% lower in IUGR ($P < 0.05$). Because protein breakdown and leucine oxidation rates were similar between groups, protein synthesis and accretion rates were 36% and 55% lower in the IUGR fetus, respectively ($P < 0.05$). Hindlimb linear growth rates in IUGR were 22% slower compared to CON ($P < 0.05$) (Fig. 3A). Phenylalanine tracers with staggered start times followed by a muscle biopsy showed a similarly lower FSR of 34% in IUGR *vs.* CON ($P < 0.05$) (Fig. 3B). FSR was higher in males compared to females

(males 0.86 ± 0.06, females 0.60 ± 0.07 % hr^{-1} $P < 0.05$), without a significant interaction between groups. The cross-sectional area of both MHC type I and type IIa myo-fibres within the tibialis anterior, FDS and biceps femoris muscles was lower in IUGR compared to CON (Fig. 3*C*).

Nutrient-oxygen quotients

The glucose-oxygen quotient tended to be higher ($P = 0.09$) and the lactate-oxygen quotient was increased by two-fold ($P < 0.05$), indicating increased glucose uptake and increased lactate output per mole of oxygen consumed by the IUGR hindlimb (Fig. 4*A*). The total amino acid-oxygen quotient was 44% lower in IUGR ($P < 0.05$) (Fig. 4*A*); thus the sum of glucose, lactate and amino acid-oxygen quotients overall was lower in IUGR compared to CON ($P < 0.05$) (Fig. 4*B*). The glucose + lactate-oxygen quotient, however, was not different between IUGR and CON (Fig. 4*B*). The sums of all of the oxidizable substrates are shown graphically in Fig. 4*C*.

Relationships between substrate concentrations, substrate uptake rates and hindlimb weight

Correlations between all blood gas values, substrates and hormone concentrations and fetal hindlimb weight are shown in Table 3. Fetal substrates and hormones showing the strongest correlations with hindlimb weight are indicated in Fig. 5 and include O_2 saturation ($r^2 = 0.80$, $P < 0.0001$), glucose ($r^2 = 0.68$, $P < 0.0001$), IGF-1 ($r^2 = 0.80$, $P < 0.0001$), insulin ($r^2 = 0.40$, $P < 0.005$) and norepinephrine ($r^2 = 0.59$, $P < 0.0001$). Oxygen uptake ($r^2 = 0.78$, $P < 0.0001$), glucose uptake ($r^2 = 0.77$, $P < 0.0001$) and carbon uptake ($r^2 = 0.86$, $P < 0.0001$) rates also positively correlated with hindlimb weights (data not shown).

Discussion

The results of the present study demonstrate that the growth rates of the fetal hindlimb and skeletal muscle
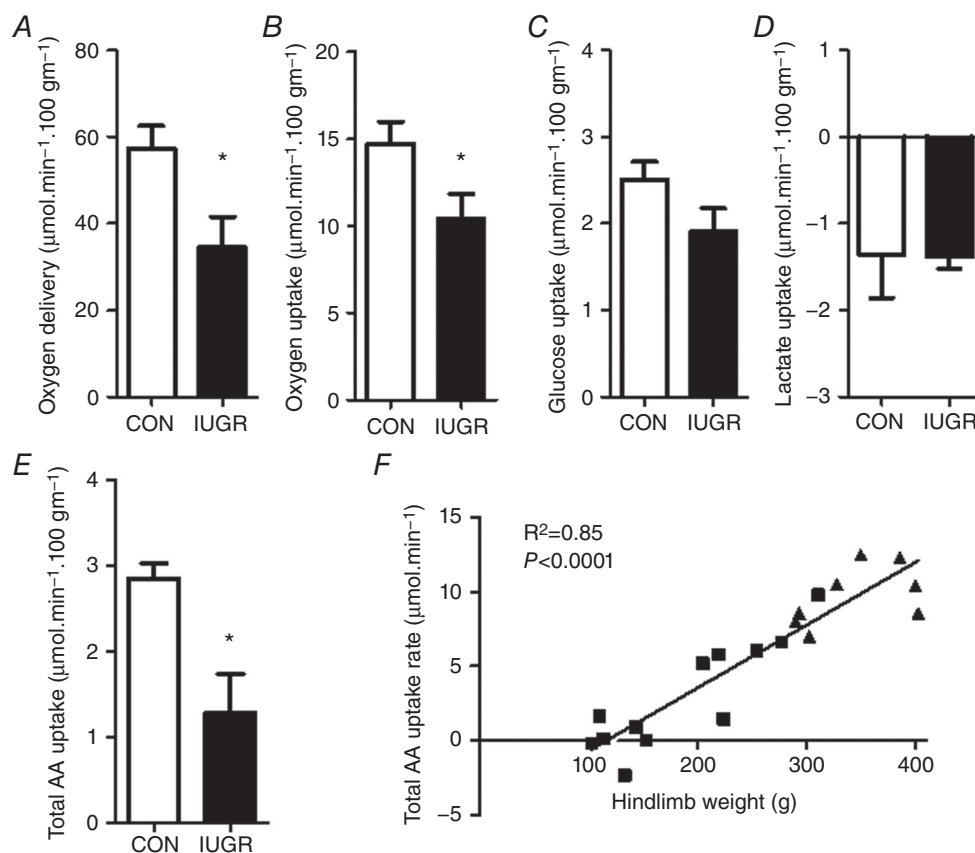
Figure 2. Net hindlimb substrate uptake rates and oxygen delivery
A, oxygen delivery rate to the hindlimb, as well as net hindlimb uptakes rates for oxygen (*B*), glucose (*C*), lactate (*D*) and total amino acids (*E*) (AA) in CON (white bars, *n* = 8) and IUGR (black bars, *n* = 11) fetal sheep at 134 days of gestation. All uptake rates and oxygen delivery normalized to 100 g of hindlimb weight. Values represent the mean ± SEM. *P < 0.05 by Student's *t* test or the Mann–Whitney test. *F*, linear relationship between total amino acid uptake rate and hindlimb weight. IUGR fetuses (squares) and CON fetuses (triangles) with correlation coefficients and *P* values are shown.

P. J. Rozance and others

are slower in the late gestation IUGR fetus compared to normally grown control fetuses. IUGR fetuses had slower hindlimb linear growth rates, smaller hindlimbs and muscle weights, and a reduced myofibre area. We used two novel stable isotope tracer studies to assess the contribution of skeletal muscle-specific protein synthesis and accretion rates to hindlimb growth. Leucine uptake rates by the hindlimb, leucine incorporation into protein accretion and the fractional protein synthetic rate all were reduced in IUGR. Muscle protein breakdown rates and leucine oxidation rates by the hindlimb were similar between groups, which indicates that the primary driver for decreased muscle growth in IUGR was a result of lower protein synthesis and accretion rates, as opposed to increased protein breakdown and oxidation. This result contrasts with a more acute energy deficiency in which protein breakdown and the oxidation of amino acids both increase to maintain basal oxidative metabolism (Limesand *et al.* 2009). Even though the absolute hindlimb blood flow rate was lower in the IUGR group,

blood flow on a weight-specific basis was similar to CON values because of reduced hindlimb and muscle growth rates. Weight-specific oxygen delivery to the hindlimb and the oxygen consumption rate also were lower in the IUGR group. The slower growth rate of the skeletal muscle and hindlimb is probably the major mechanism that reduces the oxygen consumption in the IUGR group because the reduction matches the expected oxygen cost of growth (Kennaugh *et al.* 1987). Collectively, these results demonstrate a restriction of hindlimb and skeletal muscle growth that matches blood flow and oxygen supply on a per gram weight basis.

In the transition from the first to the second half of gestation, there is a significant decline in fetal arterial blood P_{aO_2}, O_2 saturation (Bell *et al.* 1986; Soothill *et al.* 1986) and plasma glucose concentration (Molina *et al.* 1991). The primary cause of this decline is that uterine blood flow and placental permeability to diffusional exchanges do not grow as fast as the normal fetal demand for oxygen and glucose (Meschia, 2014). In IUGR cases, the gestational
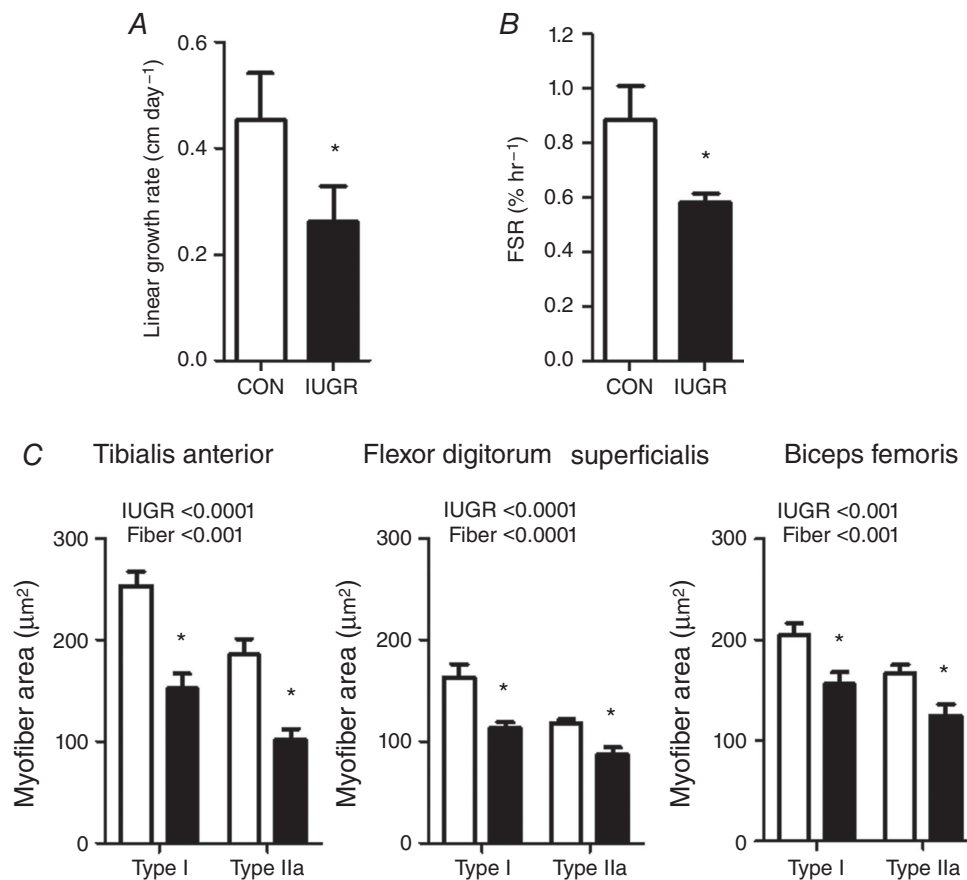

Figure 3. Hindlimb skeletal muscle growth rates and myofibre area
The hindlimb linear growth rates (*A*), FSR (*B*) and cross-sectional myofibre areas (*C*) from three hindlimb muscles were all lower in IUGR (black bars, *n* = 11–13) compared to CON (white bars, *n* = 8) fetal sheep. Values for FSR are shown as the percentage of the total protein-bound pool synthesized per hour within the biceps femoris muscle. *$P < 0.05$ by the Mann–Whitney test or a *post hoc* test comparison when ANOVA was significant for an IUGR effect.

increase of oxygen and glucose supply to the fetus does not occur to the same degree as in normal pregnancies. In more extreme IUGR cases, the fetus becomes severely compromised, with marked hypoglycaemia, hypoxia and acidosis (Thureen *et al.* 1992; Pardi *et al.* 1993; Jackson *et al.* 1995; Marconi *et al.* 1996; Regnault *et al.* 2007). The results of the present study provide evidence indicating a fetal response that limits the rate of growth of the hindlimb and other organs, such that the growth of fetal metabolic demand matches the slower increase of oxygen and nutrient supply during the latter half of gestation. We found that the total amino acid-oxygen quotient across the hindlimb and the total hindlimb amino acid uptake rate were lower in the IUGR *vs.* CON group, although

the lactate + glucose-oxygen quotient was maintained. By decreasing amino acid uptake and protein accretion rates, the fetus is able to maintain oxidative metabolism by the hindlimb at lower levels of oxygenation and glycaemia. Hindlimb growth becomes expendable to ensure survival, as demonstrated by the strong relationships between arterial O_2 saturation, glucose concentration and hind-limb weight. Because the energy cost of protein turnover and accretion in the fetal lamb accounts for ~18% of oxygen consumption (Kennaugh *et al.* 1987), the slower hindlimb growth rates probably account for the reduction in hindlimb oxygen consumption in the IUGR fetuses.
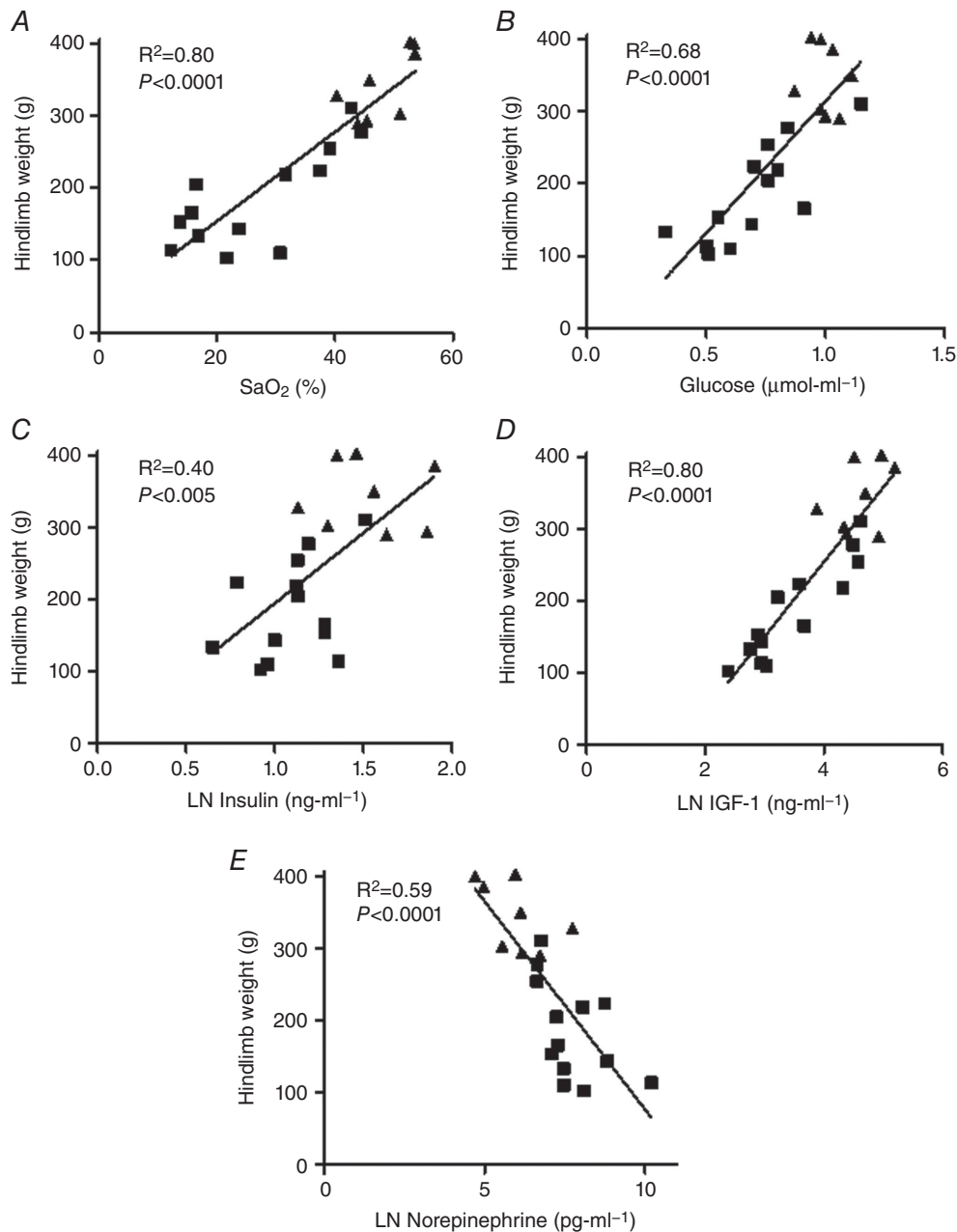
Positive associations between hindlimb weight, IGF-1 and insulin concentrations and a negative association
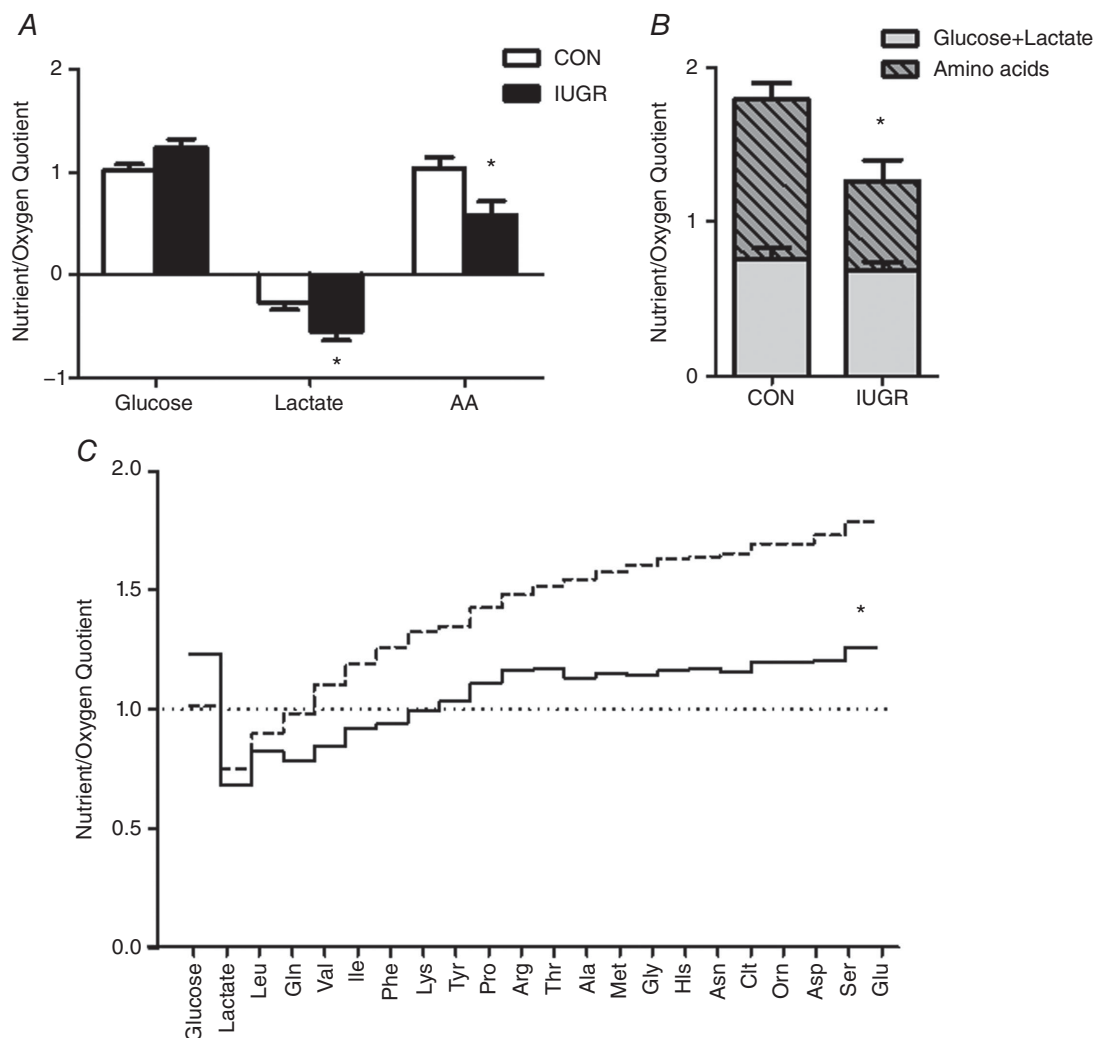
Figure 4. Nutrient-oxygen quotients by the fetal hindlimb
A, glucose, lactate and the sum of individual amino acid quotients across the hindlimb are shown for CON (white bars, *n* = 8) and IUGR (black bars, *n* = 13) fetuses. *B*, sum of glucose + lactate (grey portion of bar) *vs.* the sum of individual amino acids (grey cross-hatched portion of bar) are reduced in the IUGR fetal hindlimb. *C*, sum of individual hindlimb nutrient/oxygen quotients are presented cumulatively and demonstrate that IUGR (black continuous line) is closer to 1.0 that defines zero growth compared to CON (dashed line). *P < 0.05 by Student's *t* test.

between hindlimb weight and norepinephrine concentrations suggest that these hormones regulate fetal hindlimb growth. Norepinephrine and insulin have been implicated in providing homeostatic control of fetal oxygenation (Meschia, 2014). When growth of fetal oxygen demand exceeds growth of oxygen supply, there is a decline in fetal blood oxygen content. This decline stimulates an increase in norepinephrine in fetal blood, as demonstrated by a negative association between blood oxygen content

and norepinephrine concentrations (Limesand *et al.* 2006; Rozance *et al.* 2009b). Higher norepinephrine concentrations suppress fetal insulin secretion and lower circulating insulin concentrations (Jackson *et al.* 2000). Lower insulin concentrations, in turn, decrease fetal oxygen demand but maintain energy substrate-oxygen metabolism by slowing the rate of net protein balance and muscle growth of the hindlimb. As proof of principle, direct fetal norepinephrine infusion has been shown

Figure 5. Linear relationships between fetal factors and hindlimb weight
Fetal oxygen saturation (*A*), glucose (*B*), insulin (*C*), IGF-1 (*D*) and norepinephrine (*E*) are associated with hindlimb weight. IUGR fetuses (squares) and CON fetuses (triangles) with correlation coefficients and *P* values are shown. The natural log for insulin, IGF-1 and norepinephrine was used for the analysis.

to increase fetal oxygenation, decrease fetal insulin concentrations, and slow growth rates of skeletal and cardiac muscle (Bassett & Hanson, 1998). Conversely, lowering fetal norepinephrine concentrations by adrenal demedullation in a placental insufficiency-induced model of IUGR resulted in a partial restoration of fetal weight (Davis *et al.* 2015).

Fetal plasma IGF-1 concentrations demonstrate a much stronger correlation with hindlimb weight than does insulin, although the involvement of IGF-1 in hypoxia- or norepinephrine-mediated effects on fetal muscle growth have not been explored. Murine knockout models of IGF-1 have less muscle mass, demonstrating a direct effect of IGF-1 on muscle growth (Liu *et al.* 1993) that could explain the strong association between IGF-1 concentrations and hindlimb weight in the present study. IGF-1 has been shown to have an anabolic effect on other fetal organs such as the heart (Sundgren *et al.* 2003; Lumbers *et al.* 2009; Wang *et al.* 2011), as well as the kidney (Marsh *et al.* 2001) and liver (Eremia *et al.* 2007). It is important to note that our regression analyses correlating hormone concentrations and hindlimb weight include both IUGR and CON fetuses, with hindlimb weights ranging from 102 to 402 g. These results support a finely tuned balance between oxygen and substrate availability and circulating hormones that regulate fetal hindlimb growth in normal pregnancies, as well as those affected by IUGR.

Net total amino acid uptake rate also was reduced in IUGR fetuses and was strongly associated with hindlimb weight. Hindlimbs weighing less than 150 g (50% of normal) had negligible net amino acid uptake. This implies that, at the time of study, there was little if any growth of these hindlimbs. In addition, the sum of oxidizable carbons from substrates relative to the sum of oxygen uptake by the IUGR hindlimb was just above 1, which defines zero growth, because all carbons would be used for oxidative metabolism (Regnault *et al.* 2013). By contrast to oxygen and glucose, most amino acids showed either no association or a negative association between their arterial concentration and hindlimb weight. The exceptions were isoleucine and methionine among the essential amino acids, as well as arginine and tyrosine among the non-essential amino acids. This evidence agrees with a previous study that examined the relationship between amino acid concentrations and umbilical amino acid uptake rates in severely hypoxic IUGR fetuses (Regnault *et al.* 2013). Regnault *et al.* showed a reduction in placental permeability to oxygen and glucose that was not associated with a commensurate decrease in placental amino acid transport capacity. A reduced fetal clearance of amino acids was the dominant factor in limiting umbilical uptake rates of amino acids, based on increased fetal/maternal amino acid ratios. We now demonstrate lower inward transport of leucine into hindlimb muscle from fetal plasma and decreased intracellular leucine utilization rates by muscle, which support lower amino acid utilization by the hindlimb as a potential mechanism for the reduced clearance of amino acids by the severely hypoxic, IUGR fetus.

Plasma concentrations of essential amino acids were not significantly lower in IUGR compared to CON fetuses in the present study, which is consistent with studies in sheep and humans (Paolini *et al.* 2001; Brown *et al.* 2012; Regnault *et al.* 2013). We hypothesize that reduced skeletal muscle growth rates are not the result of lower circulating amino acid concentrations but, instead, are the result of a decreased demand for amino acids and the potential down-regulation of amino acid transport into the muscle cells because of hormonally-mediated growth inhibition (Vaughan *et al.* 2017). There were other notable changes in plasma amino acid concentrations in the IUGR fetus, including higher taurine and alanine concentrations and lower tyrosine and arginine concentrations. In starvation conditions in adults, alanine is released from the muscle (Brosnan, 2003). Increased alanine concentrations in the IUGR fetus might serve a specific purpose of routing amino acid carbon into hepatic gluconeogenesis, which is prematurely active in the IUGR fetus (Thorn *et al.* 2013). Taurine is released under conditions of severe hypoxia to serve as an osmotic regulator (Lambert *et al.* 2015). The reason for decreased arginine and tyrosine concentrations is less clear, although studies to determine the intracellular metabolic flux of these specific amino acids in IUGR fetal muscle are ongoing.

IUGR fetuses produced from multiple animal models have maintenance or even up-regulation of glucose and insulin sensitivity despite low glucose and insulin concentrations (Limesand *et al.* 2007; Wallace *et al.* 2007; Thorn *et al.* 2009). In the present study, hindlimb glucose uptake rates were not statistically different between CON and IUGR fetuses and maintained glucose uptake rates in IUGR were in the context of significantly lower glucose concentrations. Moreover, the glucose extraction efficiency was similar in both groups in the context of significantly lower plasma insulin concentrations in IUGR. These results support an increased hindlimb insulin sensitivity for glucose utilization in the IUGR fetus and also are consistent with hyperinsulinaemic-euglycaemic clamp studies in ovine IUGR fetuses that demonstrated increased insulin-stimulated glucose utilization in both the whole fetus and in the fetal myocardium (Thorn *et al.* 2013; Barry *et al.* 2016). Despite these adaptations to supply glucose to the hindlimb, skeletal muscle growth is limited, perhaps by reduced oxidation of glucose for energy production as shown in our model (Brown *et al.* 2015). Furthermore, we found an increased lactate-oxygen quotient supporting incomplete glucose oxidation, resulting in increased lactate production. The glucose + lactate-oxygen quotient was similar between groups, such that the reduction in the sum of total

oxidizable substrate was primarily the result of a reduction in the amino acid-oxygen quotient or reduced amino acid uptake per mole of oxygen consumed. These results suggest adaptations to maintain normal weight-specific oxidative metabolism of energy substrates at the expense of net protein synthesis and growth of the hindlimb.

In conclusion, evaluation of the fetal hindlimb presents a unique opportunity to determine the peripheral end-organ response in skeletal muscle to chronic reductions in amino acid, oxygen, as well as glucose supply to the fetus over gestation. In the chronic setting, a redistribution of blood flow and oxygen and nutrient substrate delivery away from less essential organ beds such as the peripheral musculature (Tchirikov *et al.* 1998; Yajnik, 2004) results in less muscle mass, a lower ponderal index and thinness at birth, which are all associated with future cardiovascular disease and insulin resistance (Barker *et al.* 1993). Both the physiological and molecular mechanisms that result in reduced fetal skeletal muscle growth have important implications for later life health. We have demonstrated that hypoxaemia, hypoglycaemia, increased norepinephrine concentrations, and reduced insulin and IGF-1 concentrations could all limit skeletal muscle and hindlimb growth, potentially by limiting amino acid uptake and utilization for protein accretion (Milley, 1994, 1997, 1998). Sex differences did not affect treatment differences, although we may not have had adequate fetal numbers to fully appreciate sex differences in the present study. These results further our understanding of the metabolic and hormonal adaptations to reduced oxygen and nutrient supply with placental insufficiency that develop to slow hindlimb growth yet support oxidative metabolism, which comprises a key survival strategy to achieve a viable fetus.

References

Akalin-Sel T & Campbell S (1992). Understanding the pathophysiology of intra-uterine growth retardation: the role of the 'lower limb reflex' in redistribution of blood flow. *Eur J Obstet Gynecol Reprod Biol* **46**, 79–86.

Allison BJ, Brain KL, Niu Y, Kane AD, Herrera EA, Thakor AS, Botting KJ, Cross CM, Itani N, Skeffington KL, Beck C & Giussani DA (2016). Fetal in vivo continuous cardiovascular function during chronic hypoxia. *J Physiol* **594**, 1247–1264.

Arroyo JA, Anthony RV & Galan HL (2008). Decreased placental X-linked inhibitor of apoptosis protein in an ovine model of intrauterine growth restriction. *Am J Obstet Gynecol* **199**, 80–88.

Baker J, Workman M, Bedrick E, Frey MA, Hurtado M & Pearson O (2010). Brains versus brawn: an empirical test of Barker's brain sparing model. *Am J Hum Biol* **22**, 206–215.

Barker DJ, Osmond C, Simmonds SJ & Wield GA (1993). The relation of small head circumference and thinness at birth to death from cardiovascular disease in adult life. *BMJ* **306**, 422–426.

Barry JS, Rozance PJ, Brown LD, Anthony RV, Thornburg KL & Hay WW Jr (2016). Increased fetal myocardial sensitivity to insulin-stimulated glucose metabolism during ovine fetal growth restriction. *Exp Biol Med (Maywood)* **241**(8), 839–847.

Bassett JM & Hanson C (1998). Catecholamines inhibit growth in fetal sheep in the absence of hypoxemia. *Am J Physiol Regul Integr Comp Physiol* **274**, R1536–R1545.

Bell AW, Kennaugh JM, Battaglia FC, Makowski EL & Meschia G (1986). Metabolic and circulatory studies of fetal lamb at midgestation. *Am J Physiol Endocrinol Metab* **250**, E538–E544.

Bell AW, Wilkening RB & Meschia G (1987). Some aspects of placental function in chronically heat-stressed ewes. *J Dev Physiol* **9**, 17–29.

Biolo G, Chinkes D, Zhang XJ & Wolfe RR (1992). Harry M. Vars Research Award. A new model to determine in vivo the relationship between amino acid transmembrane transport and protein kinetics in muscle. *JPEN J Parenter Enteral Nutr* **16**, 305–315.

Biolo G, Gastaldelli A, Zhang XJ & Wolfe RR (1994). Protein synthesis and breakdown in skin and muscle: a leg model of amino acid kinetics. *Am J Physiol Endocrinol Metab* **267**, E467–E474.

Boyle DW, Meschia G & Wilkening RB (1992). Metabolic adaptation of fetal hindlimb to severe, nonlethal hypoxia. *Am J Physiol Regul Integr Comp Physiol* **263**, R1130–R1135.

Brain KL, Allison BJ, Niu Y, Cross CM, Itani N, Kane AD, Herrera EA & Giussani DA (2015). Induction of controlled hypoxic pregnancy in large mammalian species. *Physiol Rep* **3**, E12614.

Brosnan JT (2003). Interorgan amino acid transport and its regulation. *J Nutr* **133**, 2068S–2072S.

Brosnan JT & Brosnan ME (2006). Branched-chain amino acids: enzyme and substrate regulation. *J Nutr* **136**, 207S–211S.

Brown LD, Cheung A, Harwood JE & Battaglia FC (2009). Inositol and mannose utilization rates in term and late-preterm infants exceed nutritional intakes. *J Nutr* **139**, 1648–1652.

Brown LD & Hay WW Jr (2016). Impact of placental insufficiency on fetal skeletal muscle growth. *Mol Cell Endocrinol* **435**, 69–77.

Brown LD, Rozance PJ, Bruce JL, Friedman JE, Hay WW Jr & Wesolowski SR (2015). Limited capacity for glucose oxidation in fetal sheep with intrauterine growth restriction. *Am J Physiol Regul Integr Comp Physiol* **309**, R920–R928.

Brown LD, Rozance PJ, Thorn SR, Friedman JE & Hay WW Jr (2012). Acute supplementation of amino acids increases net protein accretion in IUGR fetal sheep. *Am J Physiol Endocrinol Metab* **303**, E352–364.

Calder AG, Anderson SE, Grant I, McNurlan MA & Garlick PJ (1992). The determination of low d5-phenylalanine enrichment (0.002–0.09 atom percent excess), after conversion to phenylethylamine, in relation to protein turnover studies by gas chromatography/electron ionization mass spectrometry. *Rapid Commun Mass Spectrom* **6**, 421–424.

Davis MA, Macko AR, Steyn LV, Anderson MJ & Limesand SW (2015). Fetal adrenal demedullation lowers circulating norepinephrine and attenuates growth restriction but not reduction of endocrine cell mass in an ovine model of intrauterine growth restriction. *Nutrients* **7**, 500–516.

Economides DL, Proudler A & Nicolaides KH (1989). Plasma insulin in appropriate- and small-for-gestational-age fetuses. *Am J Obstet Gynecol* **160**, 1091–1094.

Eremia SC, de Boo HA, Bloomfield FH, Oliver MH & Harding JE (2007). Fetal and amniotic insulin-like growth factor-I supplements improve growth rate in intrauterine growth restriction fetal sheep. *Endocrinology* **148**, 2963–2972.

Gardner DS, Giussani DA & Fowden AL (2003). Hindlimb glucose and lactate metabolism during umbilical cord compression and acute hypoxemia in the late-gestation ovine fetus. *Am J Physiol Regul Integr Comp Physiol* **284**, R954–R964.

Greenough A, Nicolaides KH & Lagercrantz H (1990). Human fetal sympathoadrenal responsiveness. *Early Hum Dev* **23**, 9–13.

Jackson BT, Piasecki GJ, Cohn HE & Cohen WR (2000). Control of fetal insulin secretion. *Am J Physiol Regul Integr Comp Physiol* **279**, R2179–R2188.

Jackson MR, Walsh AJ, Morrow RJ, Mullen JB, Lye SJ & Ritchie JW (1995). Reduced placental villous tree elaboration in small-for-gestational-age pregnancies: relationship with umbilical artery Doppler waveforms. *Am J Obstet Gynecol* **172**, 518–525.

Kennaugh JM, Bell AW, Teng C, Meschia G & Battaglia FC (1987). Ontogenetic changes in the rates of protein synthesis and leucine oxidation during fetal life. *Pediatr Res* **22**, 688–692.

Lambert IH, Kristensen DM, Holm JB & Mortensen OH (2015). Physiological role of taurine–from organism to organelle. *Acta Physiol (Oxf)* **213**, 191–212.

Larciprete G, Valensise H, Di Pierro G, Vasapollo B, Casalino B, Arduini D, Jarvis S & Cirese E (2005). Intrauterine growth restriction and fetal body composition. *Ultrasound Obstet Gynecol* **26**, 258–262.

Limesand SW, Rozance PJ, Brown LD & Hay WW Jr (2009). Effects of chronic hypoglycemia and euglycemic correction on lysine metabolism in fetal sheep. *Am J Physiol Endocrinol Metab* **296**, E879–E887.

Limesand SW, Rozance PJ, Smith D & Hay WW Jr (2007). Increased insulin sensitivity and maintenance of glucose utilization rates in fetal sheep with placental insufficiency and intrauterine growth restriction. *Am J Physiol Endocrinol Metab* **293**, E1716–E1725.

Limesand SW, Rozance PJ, Zerbe GO, Hutton JC & Hay WW Jr (2006). Attenuated insulin release and storage in fetal sheep pancreatic islets with intrauterine growth restriction. *Endocrinology* **147**, 1488–1497.

Liu JP, Baker J, Perkins AS, Robertson EJ & Efstratiadis A (1993). Mice carrying null mutations of the genes encoding insulin-like growth factor I (Igf-1) and type 1 IGF receptor (Igf1r). *Cell* **75**, 59–72.

Lumbers ER, Kim MY, Burrell JH, Kumarasamy V, Boyce AC, Gibson KJ, Gatford KL & Owens JA (2009). Effects of intra-fetal IGF-I on growth of cardiac myocytes in late-gestation fetal sheep. *Am J Physiol Endocrinol Metab* **296**, E513–E519.

Marconi AM, Paolini C, Buscaglia M, Zerbe G, Battaglia FC & Pardi G (1996). The impact of gestational age and fetal growth on the maternal-fetal glucose concentration difference. *Obstet Gynecol* **87**, 937–942.

Marsh AC, Gibson KJ, Wu J, Owens PC, Owens JA & Lumbers ER (2001). Chronic effect of insulin-like growth factor I on renin synthesis, secretion, and renal function in fetal sheep. *Am J Physiol Regul Integr Comp Physiol* **281**, R318–R326.

Meschia (2014). Placental Respratory Gas Exchange and Fetal Oxygenation. In *Creasy and Resnik's Maternal-Fetal Medicine*, 7th edn, eds Creasy RK, Resnik R, Iams JD, Lockwood CL, Moore TR & Greene MF, pp. 163–174. Elsevier Saunders Inc., Philadelphia, PA.

Milley JR (1994). Effects of insulin on ovine fetal leucine kinetics and protein metabolism. *J Clin Invest* **93**, 1616–1624.

Milley JR (1997). Ovine fetal metabolism during norepinephrine infusion. *Am J Physiol Endocrinol Metab* **273**, E336–E347.

Milley JR (1998). Ovine fetal leucine kinetics and protein metabolism during decreased oxygen availability. *Am J Physiol Endocrinol Metab* **274**, E618–E626.

Molina RD, Meschia G, Battaglia FC & Hay WW Jr (1991). Gestational maturation of placental glucose transfer capacity in sheep. *Am J Physiol Regul Integr Comp Physiol* **261**, R697–R704.

Newman JP, Peebles DM, Harding SR, Springett R & Hanson MA (2000). Hemodynamic and metabolic responses to moderate asphyxia in brain and skeletal muscle of late-gestation fetal sheep. *J Appl Physiol (1985)* **88**, 82–90.

Padoan A, Rigano S, Ferrazzi E, Beaty BL, Battaglia FC & Galan HL (2004). Differences in fat and lean mass proportions in normal and growth-restricted fetuses. *Am J Obstet Gynecol* **191**, 1459–1464.

Paolini CL, Marconi AM, Ronzoni S, Di Noio M, Fennessey PV, Pardi G & Battaglia FC (2001). Placental transport of leucine, phenylalanine, glycine, and proline in intrauterine growth-restricted pregnancies. *J Clin Endocrinol Metab* **86**, 5427–5432.

Pardi G, Cetin I, Marconi AM, Lanfranchi A, Bozzetti P, Ferrazzi E, Buscaglia M & Battaglia FC (1993). Diagnostic value of blood sampling in fetuses with growth retardation. *N Engl J Med* **328**, 692–696.

Pardi G, Marconi AM & Cetin I (2002). Placental-fetal interrelationship in IUGR fetuses–a review. *Placenta* **23**(Suppl A), S136–S141.

Poudel R, McMillen IC, Dunn SL, Zhang S & Morrison JL (2015). Impact of chronic hypoxemia on blood flow to the brain, heart, and adrenal gland in the late-gestation IUGR sheep fetus. *Am J Physiol Regul Integr Comp Physiol* **308**, R151–R162.

Regnault TR, de Vrijer B, Galan HL, Wilkening RB, Battaglia FC & Meschia G (2007). Development and mechanisms of fetal hypoxia in severe fetal growth restriction. *Placenta* **28**, 714–723.

Regnault TR, de Vrijer B, Galan HL, Wilkening RB, Battaglia FC & Meschia G (2013). Umbilical uptakes and transplacental concentration ratios of amino acids in severe fetal growth restriction. *Pediatr Res* **73**, 602–611.

Rozance PJ, Crispo MM, Barry JS, O'Meara MC, Frost MS, Hansen KC, Hay WW Jr & Brown LD (2009*a*). Prolonged maternal amino acid infusion in late-gestation pregnant sheep increases fetal amino acid oxidation. *Am J Physiol Endocrinol Metab* **297**, E638–E646.

Rozance PJ, Limesand SW, Barry JS, Brown LD & Hay WW Jr (2009*b*). Glucose replacement to euglycemia causes hypoxia, acidosis, and decreased insulin secretion in fetal sheep with intrauterine growth restriction. *Pediatr Res* **65**, 72–78.

Soothill PW, Nicolaides KH, Rodeck CH & Campbell S (1986). Effect of gestational age on fetal and intervillous blood gas and acid-base values in human pregnancy. *Fetal Ther* **1**, 168–175.

Soto SM, Blake AC, Wesolowski SR, Rozance PJ, Barthel KB, Gao B, Hetrick B, McCurdy CE, Garza NG, Hay WW Jr, Leinwand LA, Friedman JE & Brown LD (2017). Myoblast replication is reduced in the IUGR fetus despite maintained proliferative capacity in vitro. *J Endocrinol* **232**, 475–491.

Sundgren NC, Giraud GD, Schultz JM, Lasarev MR, Stork PJ & Thornburg KL (2003). Extracellular signal-regulated kinase and phosphoinositol-3 kinase mediate IGF-1 induced proliferation of fetal sheep cardiomyocytes. *Am J Physiol Regul Integr Comp Physiol* **285**, R1481–R1489.

Tchirikov M, Rybakowski C, Huneke B & Schroder HJ (1998). Blood flow through the ductus venosus in singleton and multifetal pregnancies and in fetuses with intrauterine growth retardation. *Am J Obstet Gynecol* **178**, 943–949.

Thorn SR, Brown LD, Rozance PJ, Hay WW Jr & Friedman JE (2013). Increased hepatic glucose production in fetal sheep with intrauterine growth restriction is not suppressed by insulin. *Diabetes* **62**, 65–73.

Thorn SR, Regnault TR, Brown LD, Rozance PJ, Keng J, Roper M, Wilkening RB, Hay WW Jr & Friedman JE (2009). Intrauterine growth restriction increases fetal hepatic gluconeogenic capacity and reduces messenger ribonucleic acid translation initiation and nutrient sensing in fetal liver and skeletal muscle. *Endocrinology* **150**, 3021–3030.

Thureen PJ, Trembler KA, Meschia G, Makowski EL & Wilkening RB (1992). Placental glucose transport in heat-induced fetal growth retardation. *Am J Physiol* **263**, R578–R585.

Tzschoppe A, Riedel C, von Kries R, Struwe E, Rascher W, Dorr HG, Beckmann MW, Schild RL, Goecke TW, Flyvbjerg A, Frystyk J & Dotsch J (2015). Differential effects of low birthweight and intrauterine growth restriction on umbilical cord blood insulin-like growth factor concentrations. *Clin Endocrinol (Oxf)* **83**, 739–745.

Vaughan OR, Rosario FJ, Powell TL & Jansson T (2017). Regulation of Placental Amino Acid Transport and Fetal Growth. *Prog Mol Biol Transl Sci* **145**, 217–251.

Wallace JM, Milne JS, Aitken RP & Hay WW Jr (2007). Sensitivity to metabolic signals in late-gestation growth-restricted fetuses from rapidly growing adolescent sheep. *Am J Physiol Endocrinol Metab* **293**, E1233–E1241.

Wang KC, Zhang L, McMillen IC, Botting KJ, Duffield JA, Zhang S, Suter CM, Brooks DA & Morrison JL (2011). Fetal growth restriction and the programming of heart growth and cardiac insulin-like growth factor 2 expression in the lamb. *J Physiol* **589**, 4709–4722.

Wilkening RB, Boyle DW, Teng C, Meschia G & Battaglia FC (1994). Amino acid uptake by the fetal ovine hindlimb under normal and euglycemic hyperinsulinemic states. *Am J Physiol* **266**, E72–E78.

Wolfe RR & Chinkes DL (2005). Arterial-venous balance technique to measure amino acid kinetics. In *Isotope Tracers in Metabolic Research; Principles and Practice of Kinetic Analysis*, 7th edn, eds Wolfe RR & Chinkes DL, pp. 381–420. John Wiley and Sons, Inc., Hoboken, New Jersey.

Yajnik CS (2004). Obesity epidemic in India: intrauterine origins? *Proc Nutr Soc* **63**, 387–396.

Yau KI & Chang MH (1993). Growth and body composition of preterm, small-for-gestational-age infants at a postmenstrual age of 37–40 weeks. *Early Hum Dev* **33**, 117–131.

Additional information

Competing interests

The authors declare that they have no competing financial interests.

Author contributions

PJR, SRW, DAG, MCG, MSM, WWH, RBW and LDB contributed to design of the work. PJR, LZ, SRW, DAG, BS, WWH, RBW and LDB contributed to acquisition of data. PJR, LZ, SRW, DAG, MCG, MSM, GM, WWH, RBW and LDB contributed to analysis and interpretation of data. LDB drafted the paper. PJR, LZ, SRW, DAG, BS, MCG, MSM, GM, WWH and RBW revised the paper critically for important intellectual content. All authors approved the final version of the work submitted for publication and agree to be accountable for all aspects of this work.

Funding